



HAL
open science

A model based predictive tool for fire safety intumescent coatings design

Mathieu Gillet, Laetitia Perez, Laurent Autrique

► To cite this version:

Mathieu Gillet, Laetitia Perez, Laurent Autrique. A model based predictive tool for fire safety intumescent coatings design. *Fire Safety Journal*, 2019, 110. hal-02507088

HAL Id: hal-02507088

<https://univ-angers.hal.science/hal-02507088>

Submitted on 21 Jul 2022

HAL is a multi-disciplinary open access archive for the deposit and dissemination of scientific research documents, whether they are published or not. The documents may come from teaching and research institutions in France or abroad, or from public or private research centers.

L'archive ouverte pluridisciplinaire **HAL**, est destinée au dépôt et à la diffusion de documents scientifiques de niveau recherche, publiés ou non, émanant des établissements d'enseignement et de recherche français ou étrangers, des laboratoires publics ou privés.



Distributed under a Creative Commons Attribution - NonCommercial 4.0 International License

A model based predictive tool for fire safety intumescent coatings design

Mathieu Gillet¹, Laetitia Perez², Laurent Autrique³

¹DGA/DT/TA/MT/MTO, 10 rue des fours solaires, BP 59, 66121 Font-Romeu, France, mathieu.gillet@intradef.gouv.fr, +33 (0)468 307 688

²LARIS, University of Angers, 62 avenue notre dame du lac, 49000 Angers, France, laurent.autrique@univ-angers.fr, +33 (0)244 687 518

³LARIS, University of Angers, 62 avenue notre dame du lac, 49000 Angers, France, laurent.autrique@univ-angers.fr, +33 (0)244 687 518, corresponding author

Abstract

In order to improve structures survivability, intumescent paints provide an attractive alternative to insulating materials. Such protective coatings provide an efficient thermal protection due to their swelling properties when exposed to thermal aggressions. The key-goal for safety aspects is to determine which initial paint thickness has to be applied in order to satisfy thermal safety requirements. Thus, if all the thermo physical properties of the intumescent paint are accurately known, the development of a numerical predictive tool could offer a solution for safety recommendations. A numerical design of experiment is proposed. Response surfaces are determined and optimal initial paint thickness can be found using D-optimum design. The optimal thickness is validated in simulated specific accidental configurations using a Solar Furnace.

Key words: High temperature, Fire safety, Mathematical model, Partial differential equations, Numerical design of experiment.

Nomenclature

Symbol	Value	Unit	Description
d		m	Distance to the fireball
e		m	Steel substrate thickness
f		m	Ablative layer position
g		m	Growing layer position
h	10	$W.m^{-2}.K^{-1}$	Convective heat exchange coefficient

k_f	$2 \cdot 10^{12}$	s^{-1}	Pre-exponential factor
k_g	35	dimensionless	Swelling coefficient
r	see Table I.	m	Fireball radius
t		s	Time variable
x		m	Space variable
C_{steel}	475	$J.kg^{-1}.K^{-1}$	Steel specific heat
C_{abla}	1884	$J.kg^{-1}.K^{-1}$	Ablative layer specific heat
C_{grow}	1884 if $\theta < \theta_{car}$ 1005 if $\theta \geq \theta_{car}$	$J.kg^{-1}.K^{-1}$	Growing layer specific heat
E	$1.5 \cdot 10^5$	$J.mol^{-1}$	Activation energy
H	see Table I.	m	Fireball height
L_v	$5 \cdot 10^5$	$J.kg^{-1}$	Vaporization enthalpy
M		kg	Mass loss
R	8.32	$J.mol^{-1}.K^{-1}$	Universal gas constant
T		s	Simulation duration
Greek symbol	Value	Unit	Description
α_{grow}	0.1	dimensionless	Front face absorptivity
ϵ_{grow}	0.9	dimensionless	Front face emissivity
ϵ_{steel}	0.9	dimensionless	Back face emissivity
Φ		$W.m^{-2}$	Heating flux density
λ_{steel}	44.5	$W.m^{-1}.K^{-1}$	Steel thermal conductivity
λ_{abla}	0.12	$W.m^{-1}.K^{-1}$	Ablative layer thermal conductivity
λ_{grow}	0.12 if $\theta < \theta_{car}$ 0.08 if $\theta \geq \theta_{car}$	$W.m^{-1}.K^{-1}$	Growing layer thermal conductivity
ρ_{steel}	7850	$kg.m^{-3}$	Steel density
ρ_{abla}	1000	$kg.m^{-3}$	Ablative layer density
ρ_{grow}	1000 if $\theta < \theta_{car}$ 50 if $\theta \geq \theta_{car}$	$kg.m^{-3}$	Growing layer density
σ	$5.67 \cdot 10^{-8}$	$W.m^{-2}.K^{-4}$	Stefan-Boltzmann constant
θ		K	Temperature
θ_{ext}	290	K	Ambient temperature
θ_v	483	K	Pyrolysis temperature
θ_{car}	553	K	Carbonization temperature

1. Introduction

Thermal aggressions induced by explosions or fires are common threats on the battlefield. In order to improve the survivability of structures exposed to intense heat fluxes, the use of combined active and passive protection systems can be a valuable solution. Among passive protections, intumescent paints provide an alternative to usual materials (reflecting plates, insulating, ablative coatings...), see for example [1]. In fact, such coatings are particularly efficient and can be applied on different substrates as for example metals, woods, clothes or polymers [2, 3]. Such versatility is quite attractive and these paints are widely used as fire retardants in many civil applications for buildings or vehicles safety purposes [4]. In a military framework they are also used for missiles or munitions protection. Intumescent coatings have the ability to swell up when they are exposed to thermal aggressions (fire, thermal waves induced by explosion, etc.), developing a multi-layered coating. The first layer, made of ablative paint, melts into a viscous reactive layer which releases gases and swells up because of bubbles movement. This endothermic reaction ends when the thermal aggression ceases to occur or when the ablative layer vanishes. If the reactive layer's exposed face reaches a temperature threshold, it turns into a solidified carbonaceous layer. This thick porous layer is constituted mainly of air and provides an efficient insulating protection. The complexity of involved phenomena makes the development of a comprehensive predictive numerical tool (based on mechanical, chemical, optical, and thermal laws) difficult [5]. Several approaches have been recently investigated [6, 7]. It has been exhibited in [8] that a thermal model linked to grey-box models taking into account the coupled phenomena can be efficient enough to simulate temperature behaviour of coated materials and transformations of the coating (ablation and swelling). Based on physical considerations, a mathematical model (ordinary differential equations ODE and partial differential equations PDE) has been previously developed [9] and both system temperature and

coating mass loss evolution can be predicted. The model structure has been validated for thermal fluxes occurring in violent, brief explosions and in several fire configurations. Identification of several key-parameters has been investigated in [10] or in [11] since while steel substrate characteristics are well-known; those of the intumescent layers (carbonaceous, viscous and ablative) have to be carefully considered, regarding the lack of precision of the values available in literature. The main objective of the proposed communication is to develop a predictive tool in order to estimate the virgin paint thickness required in calibrated accidental scenarios (investigated hazard have to be realistic: radiative fluxes consecutive to fires, thermal waves created by sudden explosions, aggression duration, blast effect, etc.). Our approach is devoted to initial thickness optimization and is relevant only if all the input parameters of the mathematical model are known precisely and if the conditions of the accident are well informed. For a perfectly controlled painting and a well-defined accident scenario, a thickness can be proposed according to the needs of protection. But if the painting is poorly known and if the proposed scenario is not representative of reality then our approach cannot be adapted.

Numerical resolution of PDE & ODE is performed using Matlab solver. Among model inputs required for simulation, virgin paint thickness is crucial (since final carbonaceous layer thickness depends on initial paint thickness). The key-goal for safety aspects is to determine which initial paint thickness has to be applied in order to satisfy safety requirements. Inversion of the mathematical model is not suitable in an experimental context due to its inherent mathematical complexity.

A numerical design of experiment (NDOE) is then proposed in order to use the mathematical model as a valid simulation of the real processes. Then NDOE factors are mainly focused on hazardous scenarios, initial paint thickness, coated materials, etc. Investigated NDOE outputs

have to describe the safety aspects of the coated material (munitions, fuel tank, etc.). Using such approach, response surfaces are determined and optimal condition (initial paint thickness) can be found in order to satisfy thermal safety requirements using for example D-optimum design.

The communication is organized as follows: in the next section, the mathematical model is briefly described and several specific model inputs are highlighted. In the third section, calibrated accidental scenarios are presented and relevant model outputs are listed. Then the numerical design of experiment is exposed and results are given. Optimization procedure in order to obtain experimental specification for virgin coating thickness is also presented in the fifth section. Several scenarios are then tested in two accidental configurations (fire, boiling liquid expanding vapor explosion) using the Main Solar Furnace [12]. Concluding remarks and outlooks are suggested in the last section.

2. A model of intumescence phenomena

In this section, a simplified version of the mathematical model developed in [8] is briefly exposed. Numerous studies are related to intumescent coating modelling and the following references can be proposed: [2], [5], [7], [13-27]) A system of non-linear PDE describing the evolution of the system (intumescent coating and metallic substrate) during an aggression has been developed. This approach accounts for the swelling process, the heat transfers in the reactive coating and in the substrate. The system is composed of three distinct layers (figure 1):

- The first layer is the underlying substrate with fixed boundaries (space variable $x \in]0, e[$) where e is the substrate thickness.
- The second layer is the virgin paint, which upper boundary regresses during the ablation process, until it is fully consumed ($x \in]e, f(t)[$), where $t \in [0, T]$ is the time variable.

- The third layer is the growing part. When the reaction starts, its upper boundary moves upwards while the lower boundary follows the regression of the ablative layer. The solidified char layer is considered as a part of the global growing layer. It appears beyond a specified temperature threshold, and is modelled by the specification of new thermal properties for the coating. The carbonaceous layer growth is irreversible ($x \in]f(t), g(t)[$).

The system's evolution described by the model basically follows these steps:

- Initially, at $t = t_0 = 0$, the system consists of the substrate and the intumescent paint.
- At t_1 , under the effect of the radiative aggression, the ablation of the top of the intumescent coating starts, gases are released, causing the reactive layer to swell up.
- At t_2 , the top of the swelling reactive layer begins to turn into a solid char zone. The ablative layer keeps regressing.
- At t_3 , the non reactive char layer keeps growing, consuming an increasing amount of reactive material.
- At t_4 , the original intumescent coating is totally ablated.
- At t_5 , the coating stops swelling. The only remaining material is the solidified char layer.

As explained above, the description of the full system can be achieved by modeling only three layers, including the substrate. The one-dimensional approximation is justified by the direction of boundaries movement orthogonal to the steel plate and by the specific configuration for which lateral boundary effects can be neglected.

2.1 Ablative layer evolution

Experimental studies show that the front face temperature of the sample exposed to intense heat tends to a temperature threshold θ_v , corresponding to a vaporization temperature, which depends

on the type of intumescent coating. Local mass losses $M(\theta(x,t))$ in $(\text{kg.m}^{-3}.\text{s}^{-1})$ are described by an empirical law based on an Arrhenius type expression considering any points between e (the substrate's top face) and $f(t)$ (the ablative coating's top face), at any time t :

$$M(\theta(x,t)) = \begin{cases} 0 & \text{for } \theta(x,t) < \theta_v \\ -\rho_{abla} k_f \exp\left(\frac{-E}{R\theta(x,t)}\right) & \text{for } \theta(x,t) \geq \theta_v \end{cases} \quad \forall (x,t) \in]e, f(t)[\times [0, T] \quad (1)$$

where ρ_{abla} in (kg.m^{-3}) is the density of the ablative material, k_f in (s^{-1}) is the pre-exponential factor, E in (J.mol^{-1}) is the activation energy of the pyrolysis reaction, R in $(\text{J.mol}^{-1}.\text{K}^{-1})$ is the universal gas constant and $\theta(x,t)$ is the temperature. The pyrolysis front's velocity can be determined by the same method:

$$\dot{f} = - \int_e^{f(t)} \frac{M(\theta(x,t))}{\rho_{abla}} dx \quad (2)$$

with \dot{f} in (m.s^{-1}) the regression velocity of the ablative layer's upper boundary.

2.2 Reactive layer evolution

The reactive layer growth is due to pyrolysis gases release from the ablative coating. Let us consider that the swelling process induced by the pyrolysis gas flow is related to the local loss and to the pyrolysis front velocity. The following equation is proposed to evaluate the time dependent position of the swelling layer's upper boundary:

$$\forall t \in [0, T] \quad \dot{g} = k_g \dot{f} \quad (3)$$

The highly porous nature of the carbonaceous layer provides important insulating properties to the whole system, which ensures the substrate's protection. The transition between reactive layer and char layer is specified by the material's carbonisation temperature θ_{car} in (K) beyond which

char layer thermal properties have to be taken into account [28]. Once the evolution of the free boundaries $f(t)$ and $g(t)$ are modelled, the whole system's thermal state can be described.

2.3 Thermal model

Heat transfers in the layers (steel plate, ablative layer, growing layer) are described by the following non linear system of partial differential equations (4–6) where C_i , ρ_i and λ_i are respectively the specific heat ($\text{J.kg}^{-1}.\text{K}^{-1}$), density (kg.m^{-3}) and thermal conductivity ($\text{W.m}^{-1}.\text{K}^{-1}$) of each layer. Determining the thermal conductivity of intumescent coating is a key goal for researcher investigating thermal transfer based on conductive, radiative and convective considerations. Moreover, bubbles in viscous subdomain induce turbulent movements in the fluid. Last but not least, gas and smokes released at high pressures in the porous medium induce a great complexity. Thus a precise estimation of thermal conductivity in intumescent layers is still an open problem. Moreover, there exists a wide variety of intumescent paint (paint manufacturers are numerous as well as the intumescent composition which is often secret) and each thermal conductivity depends on the investigated systems. Numerous references can be considered (such as for example [5,10,17,18,23,29]).

One can notice in equation (5) that the pyrolysis reaction in the ablative layer needs an amount of energy related to the coating's vaporization enthalpy L_v in (J.kg^{-1}).

$$\left\{ \begin{array}{l} \rho_{steel} C_{steel} \frac{\partial \theta(x,t)}{\partial t} - \lambda_{steel} \Delta \theta(x,t) = 0 \quad \forall (x,t) \in]0, e[\times]0, T[\quad (4) \\ \rho_{abla} C_{abla} \frac{\partial \theta(x,t)}{\partial t} - \lambda_{abla} \Delta \theta(x,t) = -L_v M(\theta(x,t)) \quad \forall (x,t) \in]e, f(t)[\times]0, T[\quad (5) \\ \rho_{grow} C_{grow} \frac{\partial \theta(x,t)}{\partial t} - \lambda_{grow} \Delta \theta(x,t) = 0 \quad \forall (x,t) \in]f(t), g(t)[\times]0, T[\quad (6) \end{array} \right.$$

Boundary condition on the heated face ($x = g(t)$) and on the back face ($x = 0$) are given in equation (7) and (8) where h in ($\text{W.m}^{-2}.\text{K}^{-1}$) is the convective heat exchange coefficient, θ_{ext} in (K) is the ambient temperature, ε_{grow} is the emissivity of the heated surface while ε_{steel} is the steel surface emissivity, σ in ($\text{W.m}^{-2}.\text{K}^{-4}$) is the Stefan-Boltzmann constant, α_{grow} is the absorptivity of the heated growing surface and $\Phi(t)$ in (W.m^{-2}) is the heating flux.

$$x = g(t), \forall t \in [0, T] \quad ;$$

$$-\lambda_{grow} \frac{\partial \theta(x, t)}{\partial x} = h(\theta(x, t) - \theta_{ext}) + \varepsilon_{grow} \sigma (\theta^4(x, t) - \theta_{ext}^4) - \alpha_{grow} \Phi(t) \quad (7)$$

$$\lambda_{steel} \frac{\partial \theta(0, t)}{\partial x} = h(\theta(0, t) - \theta_{ext}) + \varepsilon_{steel} \sigma (\theta^4(0, t) - \theta_{ext}^4) \quad ; \quad x = 0, \forall t \in [0, T] \quad (8)$$

Initial condition is:

$$\theta(x, 0) = \theta_{ext} \quad , \quad f(0) = e \quad , \quad g(0) = e \quad ; \quad \forall x \in [0, e] \quad (9)$$

Both interfaces (steel / ablative coating and ablative coating / growing layer) are assumed to be perfect contacts. Therefore, the hypothesis of gradients and temperature continuity is taken into account.

For the considered intumescent paint, thermophysical parameters are given in the nomenclature. For each of the investigated intumescent systems, it is crucial to accurately identify all the input parameters of the model. Such requirement is crucial because uncertainties about these parameters lead to an error in the temperature predictions and therefore to the recommendations concerning the initial thickness. Once all the model input parameters fixed, a finite difference method is numerically implemented in order to predict temperature evolution $\theta(x, t)$, carbonaceous layer growth $g(t)$ and mass loss $M(t)$ in the intumescent ablative layer.

However, in order to determine the initial paint thickness, inversion of the previous non linear PDE system (1–9) is quite difficult. Let us consider in the following section several calibrated accidental scenarios.

3. Calibrated accidental scenarios

3.1 Fire

Several heat fluxes can be considered in order to describe thermal aggressions induces by fire:

- Standard static fire: $\Phi(t) = \Phi_{\min} = 5 \cdot 10^4 \text{ W.m}^{-2}$
- Intense static fire: $\Phi(t) = \Phi_{\max} = 2 \cdot 10^5 \text{ W.m}^{-2}$
- Dynamic fire: $\Phi(t) = \begin{cases} t \frac{\Phi_0}{t_f} & \text{if } t \leq t_f \\ \max\left(0, \left(2 - \frac{t}{t_f}\right)\Phi_0\right) & \text{if } t > t_f \end{cases}$, at $t = t_f$, heat flux is maximum

(equal to Φ_0) and at $t = 2t_f$, fire is extinguished ($2t_f \leq T$).

3.2 BLEVE: Boiling Liquid Expanding Vapour Explosion

A BLEVE is caused by the destruction of a pressurized tank holding a liquid which temperature exceeds its boiling point at atmospheric pressure. The tank destruction, leading to the depressurization of its content, can be caused by a bullet impact, exposition to a fire, material fatigue or corrosion. If the tank's content is a flammable product such as propane or butane, the explosion can result in the apparition of a fireball. A typical and well-known BLEVE is the explosion of a vehicle's LPG tank, which consequences are potentially deadly.

The BLEVE phenomenon can be decomposed in five steps:

- Step 1 – overpressure wave generated by the depressurization of the content's gaseous phase due to the tank's explosion. It is followed by a depression wave. Fragments can be projected several hundred meters away from the tank.
- Step 2 – release of a droplets cloud which vaporizes adiabatically while the pressure inside the cloud decreases. This vaporization goes on until the cloud's pressure equals the ambient pressure. In this phase, released vapour hardly mixes with surrounding air. A new overpressure wave is emitted.
- Step 3 – both overpressure waves have left the cloud, which keeps expanding because of its radial momentum. This expansion starts slowing down because of the growing quantity of air driven inside the turbulent mix. When the radial speed of expansion reaches the average velocity of the swirls, the remaining cloud's growth is only caused by turbulence effects.
- Step 4 – fireball appears. The ignition occurs nearby the cloud centre. The fireball's expansion stops when the whole cloud is inflamed. The velocity of this expansion equals the propagation speed of the flame inside the turbulent mix.
- Step 5 – the hemispheric fireball rises up and takes a spherical shape. Combustion goes on in the fireball, but it stops expanding because the air needed for combustion is already inside the cloud. The propellant is then supplied by the liquid droplets.

The fireball keeps rising up with constant velocity and volume, and finally takes a characteristic mushroom shape. Due to the apparition of burnt material (black spots), the apparent flame surface and the radiated heat flux then start decreasing, until total extinction.

The radiative heat emitted by the fireball is potentially the most dangerous effect of BLEVE, causing more damage and casualties than the projected fragments and the shockwaves. However, it is obvious that if the material to be protected is too close to the explosion then the pressure

wave can damage the carbonaceous layer if it has already developed. If the explosion (short and intense) takes place before the fire and the virgin layer is not reached by the projected fragments then the intumescent protection can play its role and the swelling can be obtained. We consider in the BLEVE scenario that the coated equipment is not damaged by the fugitive overpressure wave if the distance between the material and the explosion is sufficiently large, that the explosion is not too powerful and that its duration is brief. If this is not the case, it is clear that an intumescent protection (and its carbonaceous layer that is very fragile in the face of erosive forces) is not appropriate and that our approach is no longer relevant.

Several mathematical models were developed in [30-35] in order to describe the evolution of heating flux generated by the fireball. In the following, the fireball evolution, in terms of height, diameter, and emittance is investigated. This model considers the three following steps for the development of the fireball:

- Expansion phase: $t \in [0, \tau_1]$. During this cloud ignition phase, the fireball's radius and emittance increase linearly until their respective maximal values.
- Combustion phase $t \in [\tau_1, \tau_2]$. The fireball's lifetime, from its ignition to the beginning of its extinction, is considered as equal to the combustion time of the droplets generated when the product is released in the atmosphere. Indeed, the droplets inflamed at the beginning of the phenomenon are already consumed. During this phase, the temperature of the fireball is supposed to decrease linearly between its maximal value and its initial extinction temperature. The initial extinction temperature is calculated applying the principle of energy conservation, assuming the complete combustion of droplets (provided that a sufficient

amount of air is taken into the cloud). Final temperature is supposed equal at least to 88 % of the maximal fireball temperature (assumption made from experimental results). During this phase, the fireball's climbing speed is constant. The absence of real vertical acceleration is due to the air dragged by the fireball, which cools down as it rises up. Otherwise, the fireball's vertical speed would increase significantly because of an important difference of temperature with the surrounding air. Furthermore, the fireball's size is supposed to stay constant during its elevation.

- Extinction phase $t \in [\tau_2, \tau_3]$. The extinction is complete when the last droplets, which inflamed when the fireball was at maximal temperature (end of the expansion phase), are consumed. During this last phase, the fireball's diameter is supposed to decrease linearly while its emittance is assumed to be constant. Finally, the fireball stops rising up.

The heat flux $\Phi(t)$ received by a target at distance d in [m] from the fireball is expressed as:

$$\Phi(t) = 0.825 \frac{r(t)^2}{(d + H(t))^2} E(t) \quad (10)$$

where $r(t)$ is the fireball radius, $H(t)$ the height, and $E(t)$ the fireball's surface emissive power (SEP). It is obvious that determination of $S = \{\tau_1, \tau_2, \tau_3, T, E_0, E_1, R_0, H_0, H_1\}$ in experimental situation is hopeless. However, considering the three main phases (expansion $t \in [0, \tau_1]$, combustion $t \in [\tau_1, \tau_2]$ and extinction $t \in [\tau_2, \tau_3]$), equations are proposed in Table I.

Heating flux presented in figure 2 corresponds to a 11 m^3 butane tank explosion. Mass of rejected product is 2 tons, rupture pressure is 15 bars, tank's filling rate is 40 %. For such accidental configuration: $E_0 = 4.4 \cdot 10^5 \text{ W.m}^{-2}$, $E_1 = 2.6 \cdot 10^5 \text{ W.m}^{-2}$, $R_0 = 37 \text{ m}$, $H_0 = 23 \text{ m}$, $H_1 = 42 \text{ m}$.

The heat flux shape drawn in figure 2 is presenting the general characters of heat flux generated by a BLEVE. Then in order to investigate BLEVE thermal effects, only distance d is modified in the following. However, in order to accurately describe each BLEVE specificity, it is obvious that appropriate parameters set S has to be previously determined.

In the following section, three scenarios are considered:

- SF: static fire,
- DF: dynamic fire,
- BSF: BLEVE occurring during a static fire (describing for example a butane tank explosion due to a fire).

4. Numerical design of experiment and model-based design

The main objective is to determine which initial coating thickness has to be painted in order to protect the metallic substrate. The methodology derived from numerical design of experiment (NDOE) is implemented. NDOE strategy is applied to numerical results (obtained with several simulations based on a finite difference method). Each run leads to a simulation, and numerical results are obtained without unknown experimental disturbances (noise). Thus, statistical analysis (for example, significance tests, determination of confidence intervals) is meaningless. Considering that the same intumescent paint is used, let us define the model input parameters. A reasonable interval for each input, where high (+) and low (−) limits, correspond to extreme values is considered.

- Factor (A): initial paint thickness $f(0) - e$,
- Factor (B): steel substrate thickness e ,
- Factor (C): time duration T for simulation,

- Factor (D): scenario SF or BSF: heat flux generated by static fire,
scenario DF: Φ_0 (maximum heat flux),
- Factor (E): scenario DF: time t_f corresponding to maximum heat flux aggression Φ_0 ,
scenario BSF: tank explosion ,
- Factor (F): scenario BSF: distance in between target and fireball d .

In Table II, factor's levels are listed.

Previous non-linear PDE system (1–9) is numerically solved considering finite element method (implemented with Comsol® combined with Matlab®) [36-37], in order to predict temperature evolution $\theta(x,t)$, carbonaceous layer growth $g(t)$ and mass loss $M(t)$. Convergence of the numerical code has been verified in order to obtain robust numerical solutions which are not affected by discretization parameters. The proposed configuration is based on 257 nodes and element types are Lagrange T2 J1. For a general presentation of the finite element method, the following references can be considered [38-39].

The main investigated model outputs are:

- Response (Y_1): temperature on the substrate back face (uncoated) at the end of the simulation $\theta(0,T)$,
- Response (Y_2): maximum temperature on the substrate back face $\max_{t \in [0,T]} \theta(0,t)$,
- Response (Y_3): intumescent coating growth.

Considering static fire (SF: 4 factors) as well as dynamic fire (DF: 5 factors) or Fire & BLEVE (BSF: 6 factors), D-optimal designs of experiment are proposed in order to investigate quadratic

models and response surface modeling. Such design and corresponding results are presented in Tables III-V.

Considering previous tables, polynomial models can be determined for (Y_1) , (Y_2) and (Y_3) in each considered scenario. Models coefficients are obtained using multilinear regression. For example, for static fire scenario, the following polynomial models are obtained:

$$Y_1 \approx 431 - 32.3A - 15.9B + 6.6C + \frac{1.34D}{1000} - 0.18AB - 0.58AC - \frac{0.54AD}{1000} + 0.55BC + \frac{0.023BD}{1000} + \frac{0.011CD}{1000} + 16.7A^2 + 0.8B^2 - 0.24C^2 + \frac{D^2}{10^9}$$

$$Y_2 \approx 384 - 29.2A - 7.3B + 12.6C + \frac{1.23D}{1000} - 0.08AB - 1.05AC - \frac{0.5AD}{1000} + 0.46BC + \frac{0.022BD}{1000} + \frac{0.003CD}{1000} + 16.7A^2 - 0.9B^2 - 0.38C^2 + \frac{1.8D^2}{10^9}$$

$$Y_3 \approx -27 - A + 14.3B - C + \frac{0.64D}{1000} + 0.74AC + \frac{0.19AD}{1000} + 0.08BC + \frac{0.002BD}{1000} + \frac{0.001CD}{1000} - 4.5A^2 - 3.9B^2 + 0.019C^2 - \frac{2.8D^2}{10^9}$$

The same multilinear regression method is considered in order to define polynomial models coefficients in case of dynamic fire (DF: 5 factors and 20 coefficients) or Fire & BLEVE (BSF: 6 factors and 27 coefficients).

Then, optimization can be performed in order to satisfy experimental requirements. Considering a given steel substrate thickness, our goal is to define the coating thickness able to protect the plate's back face for several calibrated aggressions. For practical reasons, let us consider that

temperature on steel back face has to remain under a maximum temperature (target), see examples in Tables VI-VIII.

For mechanical reasons, it is noteworthy that a huge swelling is quite fragile [40]. Thus final growth greater than 50 mm can be difficult to maintain. However, it has been observed that even if the carbonaceous layer is damaged (wind, blowing effect ...), protection can be ensured if ablative layer is not totally consumed. In order to find a relevant thickness (input A) which can fulfil the safety requirements, an optimization method is used considering that the previous polynomial models are validated. The well-known downhill simplex method [41] on the fitted response surface is implemented in order to minimize an overall desirability function that combines the individual desirability of each response.

5. Experimentation

In order to verify that previous recommendations are meaningful, experimentations have been performed using the Main Solar Furnace (figure 3) in DGA/DT/TA/MT/MTO institute (French Ministry of Defense). This device is composed of:

- a 230 m² plane heliostat (reflector) composed of 638 square mirrors reflecting solar radiation to the concentrator and the attenuator,
- a solar radiation modulator consisting of fast-moving shutters,
- a concentrator (10.75 m focal length) covering an area of 100 m².

The complete experimental setup which is able to simulate thermal effect of fire or explosion is called the Main Solar Furnace (MSF) and is detailed in reference [8]. The associated metrology (pyrometer, type K thermocouples, infrared camera, digital scale, digital video cameras) allows to measure the evolution of the swelling process, the mass losses, the radiative flux emitted by

the heated surface, the smokes emission, the temperature of the back face of the substrate, the spatial distribution of the radiative flux on the back face of the substrate ...

This solar furnace is specifically designed to reproducibly produce perfectly controlled thermal flows that can reach very high values in very short times. Thus it is very relevant to simulate the effect of the intense heat produced by fires or explosions. However, it is not developed to study the effects of pressure waves during explosions or that of additional erosive conditions during an accident.

This experimental setup is implemented in order to perform all the real tests for validation in table IX. It is important to note that each test is performed several times in order to verify that the measured maximum temperature and the measured growth at the end of the tested situation are not dramatically disturbed.

Using this original device, calibrated heating fluxes can be obtained and in accidental scenarios, thermal safety of tested samples can be estimated. A thin ($e = 1$ mm) square steel plate (10 cm x 10 cm) has been considered. Two scenarios are taken into account:

- for a static fire (constant heat flux 170 kW.m^{-2}) a maximum back face temperature equal to 550K is desired after 5 minutes,
- for a BLEVE occurring during a static fire (constant heat flux 170 kW.m^{-2} , explosion 5 minutes after the fire ignition), a maximum back face temperature equal to 550 K is desired for a steel sample at 20 m from the fireball (6 minutes after the fire ignition).

Recommendations (obtained using the model based design presented in previous section) are then compared to experimentation.

Considering Table IX, the interest of our approach is verified and the model based design seems able to propose useful recommendations for safety purposes in numerous accidental scenarios. It

is quite important to notice that the obtained polynomial models obviously depend on the intumescent system which is investigated. In [42], considering a sensitivity approach based on numerical design of experiment, key-parameters which have to be carefully estimated for our intumescent system are listed.

6. Concluding remarks

In order to ensure survivability of military equipment (i.e.: fuel tanks, ammunition, missiles, etc.) undergoing severe thermal aggressions on the battlefield such as fires or explosion induced fireballs, intumescent paints are valuable solutions because of their cost, ease of use, versatility and efficiency. The optimization of this protection requires an accurate knowledge of the amount of paint needed to meet safety requirements. For that purpose, a predictive tool was developed in order to evaluate the initial coating thickness required to achieve optimal protection in specific aggression scenarios. This tool is based upon a previously developed mathematical model which describes the overall reactive behavior of an intumescent paint layer by calculating its swelling and the heat transfers inside the coating and the underlying material. Predictions are meaningful if the thermo physical properties of the paint and substrate are accurately known and the accidental scenario is well defined.

The relevant outputs of this model are identified (back face temperature, maximal back face temperature and coating growth), and the influence of the principal input factors on these outputs are studied by means of Numerical Designs Of Experiments (NDOE) for 3 calibrated aggression scenarios: static fire, dynamic fire and BLEVE occurring during a static fire. In order to avoid a complex mathematical inversion of the whole model, polynomial models are identified to describe the outputs evolution in each of the considered scenarios. On the basis of these

polynomial models, and of protection objectives (mainly considering the coated material's back face temperature), recommended initial paint thickness are computed. These requirements are then validated experimentally, using a high temperature testing facility: the Main Solar Furnace. The tests results and the expected growths and temperatures are in good agreement, proving the efficiency of the developed predictive tool if the paint properties are accurately known and for well-defined accidental scenario.

In order to improve experimental validation and to study a wider range of accident scenarios, the effect of erosive forces could be studied. In fact, the usual intumescent paints are very fragile once the anthrax is totally inflated. To do this a specific enclosure could be developed in the solar furnace hearth in which it would be possible to simulate high winds, impacts as well as shocks and vibrations. This would make it possible to better know the behavior of the studied paints and to have recommendations of initial thickness even more adapted.

7. References

- [1] E.D. Weil, Fire-Protective and Flame-Retardant Coatings - A State-of-the-Art Review, Journal of fire sciences, Vol. **29**(3), pp. 259-296, 2011.
- [2] S. Bourbigot, , M. Le Bras, S. Duquesne and M. Rochery, Recent advances for intumescent polymers, Macromolecular Materials and Engineering, Vol. **289**(6), pp. 499-511, 2004.
- [3] M. Leca, L. Cioroianu, G. Cioroianu , G. Damian, C. Costea, and A. M. Matei, Aqueous ecological intumescent fire retardant coatings for multifunctional applications. 1. Preparation and characterization, Revue Roumaine de Chimie, Vol. **52**(8-9), pp. 745-752, 2007.

- [4] R. J. Asaro, B. Lattimer, C. Mealy, and G. Steele, Thermophysical performance of a fire protective coating for naval ship structures, *Composites part A: applied science and manufacturing*, Vol. **40**(1), pp. 11-18, 2009.
- [5] C. Di Blasi, Modeling the effects of high radiative fluxes on intumescent material decomposition, *Journal of Analytical and Applied Pyrolysis* **8** 721–37, 2004.
- [6] C. Chen, and B. Shen, A Simplified Model for Describing the Effect of Intumescent Coating to Protect Steel Under Fire Conditions, *Advanced science letters*, Vol. **4**(3), pp. 1265-1269, 2011.
- [7] G. J. Griffin, The Modeling of Heat Transfer across Intumescent Polymer Coatings, *Journal of fire sciences*, Vol. **28**(3), pp. 249-277, 2010.
- [8] M. Gillet, L. Autrique, and L. Perez, Mathematical model for intumescent coating growth: application to fire retardant systems evaluation, *Journal of physics D: Applied Physics*, Vol. **40**(3), pp. 883–899, 2007.
- [9] S. Rodier, , L. Autrique, L. Perez, N. Ramdani and J. J. Serra, Fire protective coatings evaluation : tests and modelization based on a non linear partial differential equations system, IMACS 17th world congress, Paris, France, 2005.
- [10] J. E. J. Staggs, Thermal conductivity estimates of intumescent chars by direct numerical simulation, *Fire safety Journal*, Vol. **45**(4), pp. 228-237, 2010.
- [11] L. Perez, L. Autrique, and M. Gillet, Implementation of a conjugate gradient algorithm for thermal diffusivity identification in a moving boundaries system, *Journal of Physics: Conference Series*, Vol. **135**(1), pp. 1–9, 2008.
- [12] L. Autrique, L. Perez, and M. Gillet, Analysis of intumescent systems: model and experimentations, proceedings of the European Control Conference 07, KOS, Greece, 2007.

- [13] D.E. Cagliostro, S.R. Riccitiello, K.J. Clark, and A.B. Shimizu, Intumescent coating Modelling, *Journal of Fire and Flammability*, 6, pp. 205–221, 1975.
- [14] C.E. Anderson and D.K. Wauters, A thermodynamic heat transfer model for intumescent system, *International Journal of Engineering Science*, Vol. **22**(7), pp. 881–889, 1984.
- [15] J. Buckmaster, C. Anderson and A. Nachman, A model for intumescent paints, *International Journal of Engineering Science*, Vol. **24**, pp. 263–76, 1986.
- [16] L. Butler, H.R. Baum and T. Kashiwagi, Three-dimensional modeling of intumescent behaviour in fires, *Fire Safety Science – Proceedings of the 5th International Symposium (Melbourne, Australia)*, pp 523–534, 1997.
- [17] S. Duquesne, S. Bourbigot and J.M. Leroy, Modelling of heat transfer in intumescent material during combustion, *ECCE2 – 2nd European Congress of Chemical Engineering (Montpellier), France*, 1999.
- [18] J.E.J. Staggs, Approximate solutions for the pyrolysis of char forming polymers and filled polymers under thermally thick conditions, *Fire and Materials*, Vol. **24**, pp. 305–308, 2000.
- [19] K.P. Norgaard, K. Dam-Johansen, P. Catal and S. Kiil, Engineering model for intumescent coating behavior in a pilot-scale gas-fired furnace, *American Institute of Chemical Engineers AIChE Journal*, Vol. **62**(11), pp. 3947–3962, 2001.
- [20] C. Di Blasi and C. Branca, Mathematical model for the nonsteady decomposition of intumescent coatings, *American Institute of Chemical AIChE Journal*, Vol. **47**(10), pp. 2359–2370, 2001.
- [21] Y.C. Wang, U. Goransson, G. Holmstedt and A. Omrane, A Model for Prediction of Temperature in Steel Structure Protected by Intumescent Coating, based on Tests in the Cone

- Calorimeter, Fire Safety Science – Proceedings of the 8th International Symposium (Beijing, China), pp. 235-246, 2005.
- [22] F. Zhang, J. Zhang and Y. Wang, Modeling study on the combustion of intumescent fire-retardant polypropylene, *Express Polymer Letters*, Vol. **1**(3), pp. 157-165, 2007.
- [23] S. Bourbigot, M. Jimenez and S. Duquesne, Modeling Heat Barrier Efficiency of Flame Retarded Materials, Proceedings of the COMSOL Users Conference, Paris, 2006.
- [24] L. Calabrese, F. Bozzoli, G. Bochicchio, B. Tessadri, S. Rainieri and G. Pagliarini, Thermal characterization of intumescent fire retardant paints, *Journal of Physics: Conference Series*, **547**, 012005, 2014.
- [25] J. Alongi, Z. Han, S. Bourbigot, Intumescence: Tradition versus novelty. A comprehensive review, *Progress in Polymer Science*, Vol. **51**, pp. 28–73, 2015.
- [26] V.G. Zverev, V.I. Zinchenko and A. F. Tsimbalyuk, Physical and mechanical properties and thermal protection efficiency of intumescent coatings, *IOP Conf. Series: Materials Science and Engineering*, **124**, 0112109, 2016.
- [27] B.K. Cirpici, Y.C. Wang, B.D. Rogers and S. Bourbigot, A theoretical model for quantifying expansion of intumescent coating under different heating conditions, *Polymer Engineering & Science*, Vol. **56**(7), pp. 798-809, 2016.
- [28] E. Kandare, B.K. Kandola and J.E.J. Staggs, Global kinetics of thermal degradation of flame-retarded epoxy resin formulations, *Polymer degradation and Stability*, vol. **92**, pp. 1778-1787, 2007.
- [29] S., Sato, K. Oka and A. Murakami, Heat transfer behavior of melting polymers in laminar flow field; *Polymer Engineering and Science*, vol. **44**(3), pp. 423-432, 2004,

- [30] S.R. Shield, A model to Predict Radiant Heat and Blast Hazards from LPG BLEVE, AIChE 29th National Heat Transfer Conference, Atlanta, USA, pp. 139–149, 1993.
- [31] S.R. Shield, The modeling of BLEVE fireball transients, Proceedings of the 2nd European Conference on Major Hazards On and Off-shore, (Manchester -UK), IChemE Symposium Series **139**, pp. 227-236, 1995.
- [32] G.M. Makhviladze, J. Roberts and S. Yakush, Modelling the fireballs from methane releases, Fire Safety Science – Proceedings of the 5th International Symposium (Melbourne, Australia), pp. 213–224. 1997.
- [33] W.E. Martinsen, and J.D. Marx, An improved model for the prediction of radiant heat from fireballs, International Conference and Workshop on Modeling Consequences of Accidental Releases of Hazardous Materials, San Francisco, USA, September 28 - October 1, 1999.
- [34] G.M. Makhviladze and S.E.Yakush, Modelling of Formation and Combustion of Accidentally Released Fuel Clouds, Process Safety and Environmental Protection, Vol. **83**(2), March 2005, Pages 171-177, 2005.
- [35] J.A. Vílchez, M. Muñoz, J.M. Bonilla and E. Planas, Configuration factors for ground level fireballs with shadowing, Journal of Loss Prevention in the Process Industries, Vol. **51**, pp. 169-177, 2018;
- [36] W.B.J. Zimmerman, Multiphysics Modeling With Finite Element Methods, World Scientific Publishing, 2006.
- [37] R.W. Pryor, Multiphysics modeling using Comsol® v.4 – a first principles approach, Mercury Learning & Information, 2012.

- [38] D.W. Pepper and J.C. Heinrich, The finite element method – basic concepts and applications, Ed. New York: Taylor & Francis, 2006.
- [39] A.J. Baker, Finite Elements: Computational Engineering Sciences, Wiley, 2012.
- [40] I.S. Reshetnikov, M.Y. Yablokova, E.V. Potapova, N.A. Khalturinskij, V.Y. Chernyh, and L.N. Mashlyakovskii, Mechanical stability of intumescent chars, Journal of Applied Polymer Science, Vol. **67**(10), pp. 1827-1830, 1998.
- [41] J. Nelder and R. Mead, A simplex method for function minimization. The Computer Journal, Vol. **7**(4), pp. 308–313, 1965.
- [42] M. Gillet, L. Autrique, L. Perez and J.J. Serra, Parametric identification using photothermal data inversion: application to a nonlinear thermal system, Proceedings of the 2007 American Control Conference, New York City, USA, July 11-13, 2007.

Table I. Fireball characteristics.

	Surface emissive power $E(t)$	Radius $R(t)$	Height $H(t)$
expansion $t \in [0, \tau_1]$	$t \frac{E_0}{\tau_1}$	$t \frac{R_0}{\tau_1}$	$t \frac{H_0}{\tau_1}$
combustion $t \in [\tau_1, \tau_2]$	$E_0 + \frac{(E_1 - E_0)}{\tau_1 - \tau_2}(\tau_1 - t)$	R_0	$H_0 + \frac{(H_1 - H_0)}{\tau_2 - \tau_1}(t - \tau_1)$
extinction $t \in [\tau_2, \tau_3]$	E_1	$R_0 + \frac{R_0}{\tau_3 - \tau_2}(\tau_2 - t)$	H_1

Table II. Model factors levels for NDOE.

	(A)	(B)	(C)	SF or BSF (D)	DF (E)	BSF (E)	BSF (F)
(-)	1 mm	1 mm	10 min	Φ_{\min}	5 min	1 min	10 m
0	2 mm	2 mm	15 min	$\frac{1}{2}(\Phi_{\min} + \Phi_{\max})$	$\frac{15}{2}$ min	5 min	20 m
(+)	3 mm	3 mm	20 min	Φ_{\max}	10 min	9 min	30 m

Table III. NDOE and results for static fire: FS scenario

run	(A) [mm]	(B) [mm]	(C) [min]	(D) [kW.m ⁻²]	(Y ₁) [K]	(Y ₂) [K]	(Y ₃) [mm]
1	1	1	10	50	489.8	490.7	10.1
2	3	2	10	50	482.1	482.2	9.2
3	1	3	10	50	489.8	490.7	10.1
4	3	3	10	50	482.1	482.2	9.2
5	2	1	15	50	483.0	484.6	19.2
6	1	1	20	50	489.0	490.7	17.8
7	3	1	20	50	481.8	482.2	22.9
8	1	3	20	50	489.0	490.7	17.8
9	3	3	20	50	481.8	482.2	22.9
10	3	1	10	125	501.9	501.9	64.2
11	1	3	10	125	548.2	548.2	34.5
12	1	1	15	125	590.0	590.0	34.5
13	2	2	20	125	531.3	531.3	69.5
14	1	1	10	200	669.2	669.2	33.8
15	3	1	10	200	508.3	531.3	77.5
16	1	3	10	200	672.8	672.8	33.4
17	3	3	10	200	508.4	531.3	77.5
18	3	2	15	200	514.5	531.3	94.2
19	3	3	15	200	514.5	531.3	94.2
20	1	1	20	200	692.7	692.7	33.4
21	2	1	20	200	573.5	573.5	69.5
22	3	1	20	200	521.6	521.6	102.2
23	1	3	20	200	692.7	692.7	33.4
24	3	3	20	200	521.6	521.6	102.2

Table IV. NDOE and results for dynamic fire: DF scenario.

run	(A) [mm]	(B) [mm]	(C) [min]	(D) [kW.m ⁻²]	(E) [min]	(Y ₁) [K]	(Y ₂) [K]	(Y ₃) [mm]
1	2	1	10	50	5	376.8	469.0	0.0
2	3	3	10	50	5	398.8	447.0	0.0
3	1	3	15	50	5	308.2	485.7	0.9
4	3	1	20	50	5	295.8	447.0	0.0
5	1	2	20	50	5	293.6	485.7	0.9
6	1	1	10	125	5	527.0	527.0	31.7
7	3	3	15	125	5	501.3	501.3	70.5
8	3	1	10	200	5	503.7	503.7	61.9
9	2	2	10	200	5	517.5	517.5	56.7
10	1	3	10	200	5	546.7	546.7	34.5
11	1	1	15	200	5	547.9	548.0	34.5
12	2	1	20	200	5	530.7	530.7	69.5
13	1	3	20	200	5	547.2	548.2	34.5
14	3	3	20	200	5	512.4	512.4	96.1
15	1	1	10	50	7.5	479.2	512.4	2.2
16	2	3	20	50	7.5	298.8	480.0	0.1
17	1	1	20	125	7.5	534.5	534.5	34.5
18	3	2	15	200	7.5	505.9	534.5	77.5
19	1	3	10	50	10	486.7	534.5	0.6
20	3	3	10	50	10	455.1	534.5	0.0
21	3	1	15	50	10	451.8	534.5	0.0
22	1	1	20	50	10	414.3	488.4	3.2
23	3	3	20	50	10	368.3	473.6	0.0
24	3	1	10	125	10	495.2	495.2	28.4
25	1	2	10	125	10	514.0	514.0	19.6
26	1	1	10	200	10	527.1	527.1	29.8
27	3	3	10	200	10	499.2	499.2	45.8
28	2	3	15	200	10	516.0	516.0	59.4
29	3	1	20	200	10	507.7	507.7	86.7
30	1	3	20	200	10	552.1	561.3	34.5

Table V. NDOE and results for fire & BLEVE: BSF scenario.

run	(A) [mm]	(B) [mm]	(C) [min]	(D) [kW.m ⁻²]	(E) [min]	(F) [m]	(Y ₁) [K]	(Y ₂) [K]	(Y ₃) [mm]
1	1	1	10	50	1	10	508.4	530.5	29.8
2	3	1	20	50	1	10	181.8	482.0	22.7
3	2	3	10	125	1	10	519.8	519.8	63.1
4	3	3	20	125	1	10	509.5	509.5	94.0
5	3	2	10	200	1	10	508.3	508.3	77.8
6	1	1	20	200	1	10	732.6	732.6	4.2
7	3	1	10	50	5	10	490.9	494.1	33.3
8	1	3	20	50	5	10	492.5	496.0	21.2
9	1	3	10	200	5	10	734.3	753.2	3.2
10	3	3	10	50	9	10	482.1	495.0	9.1
11	1	1	20	50	9	10	491.4	491.7	18.8
12	2	2	15	125	9	10	525.0	525.0	68.3
13	1	1	10	200	9	10	739.2	753.3	3.2
14	3	1	20	200	9	10	521.0	521.0	101.9
15	2	3	20	200	9	10	570.0	570.0	69.5
16	1	2	10	50	1	20	503.0	518.5	25.7
17	2	2	20	50	5	20	485.3	488.9	29.9
18	3	3	15	200	5	20	514.2	514.2	93.8
19	3	1	10	125	9	20	502.0	514.2	65.0
20	1	3	15	200	9	20	734.3	746.9	3.2
21	3	1	10	50	1	30	482.1	737.5	9.4
22	1	3	15	50	1	30	492.6	505.9	20.2
23	1	1	20	50	1	30	492.0	505.9	23.2
24	3	3	20	50	1	30	481.8	482.2	23.0
25	3	3	10	125	1	30	502.1	502.1	65.4
26	1	1	10	200	1	30	734.3	734.3	3.2
27	3	1	20	200	1	30	521.2	521.2	102.0
28	1	3	20	200	1	30	732.6	732.6	4.2
29	1	2	10	125	5	30	550.4	550.4	34.5
30	1	1	10	50	9	30	489.8	490.7	10.1
31	2	3	10	50	9	30	483.9	484.8	12.3
32	3	1	20	50	9	30	482.0	482.2	25.0
33	1	3	20	50	9	30	489.9	490.6	18.2
34	3	2	10	200	9	30	508.1	508.1	77.0
35	2	1	15	200	9	30	543.8	543.8	69.5
36	1	1	20	200	9	30	734.3	743.4	3.2
37	3	3	20	200	9	30	521.0	521.0	101.9

Table VI. Example of recommendations for static fire scenario.

steel thickness in [mm]	<i>Experimental requirements</i>			target in [K]	<i>Recommendation</i>	<i>Expectation</i>
	heat flux in [kW.m ⁻²]	fire duration in [min]	intumescent thickness in [mm]		final growth in [mm]	
1	100	12	500	2.4	49	
1	70	20	500	1.4	30	
2	170	8	600	1.2	45	

Table VII. Example of recommendation for dynamic fire scenario.

steel thickness [mm]	<i>Experimental requirements</i>				target [K]	<i>Recommendation</i>	<i>Expectation</i>
	heat flux [kW.m ⁻²]	simulation duration [min]	time t_f [min]	intumescent thickness in [mm]		final growth [mm]	
1	120	20	10	500	1.6	46	
2	170	10	5	520	1.4	44	
2	180	10	5	500	2.4	54	

Table VIII. Example of recommendation for BSF scenario.

Steel thickness [mm]	<i>Experimental requirements</i>					Target [K]	<i>Reco.</i>	<i>Expec.</i>
	Heat flux [kW.m ⁻²]	simulation duration [min]	BLEVE time [min]	distance [m]	Intumescent thickness in [mm]		final growth [mm]	
1	100	20	1	20	500	2.4	67	
1	100	20	5	10	500	1.7	60	
1	100	20	5	10	500	1.4	56	
2	170	10	1	10	500	3.0	83	
1	170	10	6	10	500	2.5	81	
1	70	10	6	28	510	1.7	42	

Table IX. Experimental validation of recommendation.

scenario	desired	time in minutes	recommended	expected growth	measured	measured growth
	maximum temperature		paint thickness		maximum temperature	
SF	550 K	5	0.9 mm	31 mm	545 K	30 mm
BSF	450 K	6	1.2 mm	35 mm	452 K	33 mm

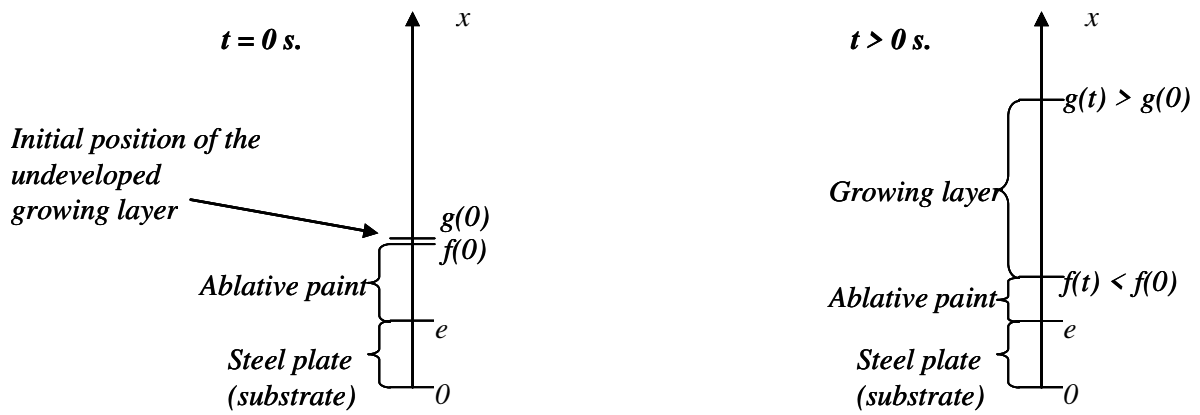


Figure 1. Domain structure before and during the reactive process.

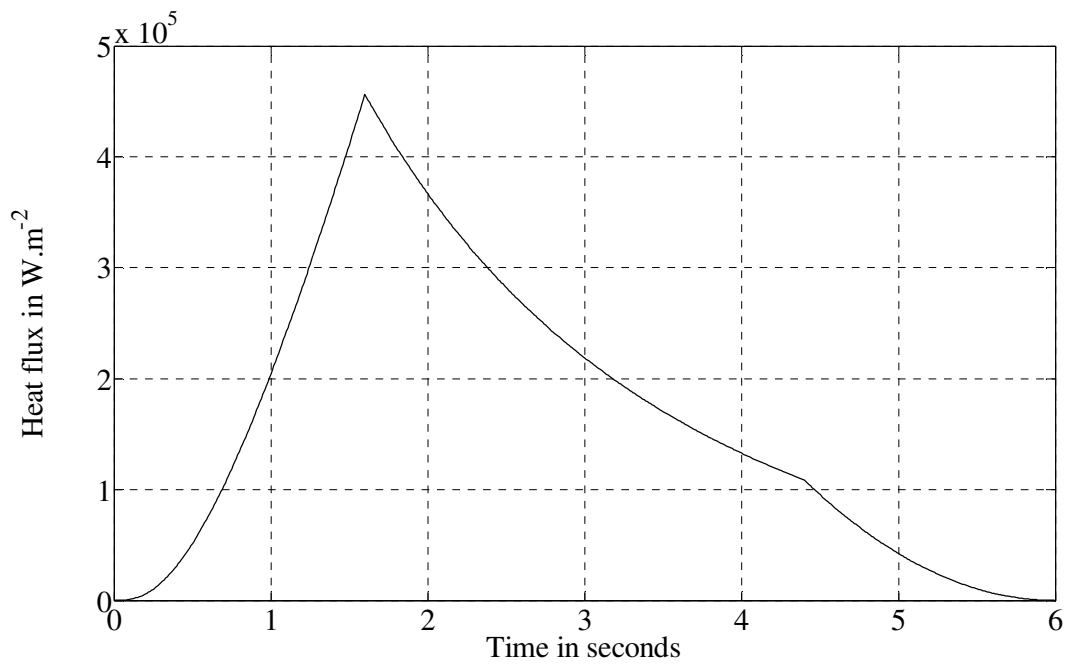


Figure 2. Example of heating flux emitted by a fireball (target 10m away from the fireball).



Figure 3. Main Solar Furnace (reflector, modulator, concentrator)

Figure captions:

Figure 1. Domain structure before and during the reactive process.

Figure 2. Example of heating flux emitted by a fireball (target 10m away from the fireball).

Figure 3. Main Solar Furnace (reflector, modulator, concentrator)